J Nanopart Res (2017) 19: 338
DOI 10.1007/s11051-017-4022-4

RESEARCH PAPER

Effects of weathering and rainfall conditions on the release of SiO_2, Ag, and TiO_2 engineered nanoparticles from paints

Xiaoran Zhang · Mingxiu Wang · Siyu Guo · Ziyang Zhang · Haiyan Li

Received: 7 January 2017 / Accepted: 12 September 2017 / Published online: 13 October 2017

Abstract Previous studies on the fate of engineered nanoparticles (ENPs) incorporated in paints mainly focused on the release of the particles as affected by a limited number of factors or monitoring their release from natural sources. In this study, the effects of four factors (i.e., weathering duration, water pH, rainfall duration and intensity) were investigated on the release of SiO_2-ENPs, Ag-ENPs, and TiO_2-ENPs from paints applied on panels. The static water immersion test showed that the concentrations of studied particles all increased with weathering duration. At low and high pH, SiO_2-ENPs and Ag-ENPs showed a higher release, while the release of TiO_2-ENPs was relatively high at low pH. With increased simulated rainfall duration, the concentration released decreased for Si, and the opposite was observed for Ag, while no obvious correlation was noted for Ti. With greater rainfall intensity, there was increasing release of all particles. In total, the releases of Ag-ENPs and TiO_2-ENPs were extremely low and within the level of 21.32–42.16 μg $L^{-1}$and 0.6–2.3 μg L^{-1}, respectively, while the values for SiO_2-ENPs were in the range of 7.5–12 mg L^{-1}. Additionally, microscopic results highlighted that SiO_2-ENPs were mainly released in the form of agglomerates, and only a small fraction was below 0.1 μm. Considering these influence factors together, conclusions may be made that weathering time and rainfall duration are more important in controlling release than water pH.

Keywords Engineered nanoparticles (ENPs) · Release · Paints · Weathering · Rainfall · Environmental and health effects · Exposure

X. Zhang · M. Wang · Z. Zhang · H. Li (✉)
Beijing Engineering Research Center of Sustainable Urban Sewage System Construction and Risk Control, Beijing University of Civil Engineering and Architecture, Beijing 100044, China
e-mail: lihaiyan@bucea.edu.cn

S. Guo
Plant Health Diagnostic Service, Elizabeth Macarthur Agricultural Institute, Woodbridge Road, Menangle, NSW 2568, Australia

Introduction

Nanoparticles, which are defined as particles having at least one dimension less than 100 nm, possess higher reactivity, strength, and conductivity compared to their bulk-sized counterparts (Majestic et al. 2010). The intense interest surrounding the economic potential of nanoparticles has given rise to engineered nanoparticles (ENPs), a new type of nanoparticles intentionally produced for use in commercial products (Majestic et al. 2010; Kai et al. 2010). One important application is the use of ENPs in paints and coatings, as they improve resistance to chemicals, erosion, abrasion, UV light, and antifouling properties (Khanna 2008). European studies roughly estimated that 10–30% of their TiO_2-ENP production, 10–30% of the Ag-ENPs, 5–10% of the CeO_x-ENPs, and 30–40% of the SiO_2-ENPs were in paints and/or related products (coatings and cleaning agents) (Piccinno et al. 2011; Mitrano et al. 2015). Due to the wide range of applications, several studies have

predicted that ENPs may end up in relevant quantities in the environment and pose potential risks (Alvarez et al. 2009; Wiesner et al. 2009; Nowack et al. 2011). Based on the estimation by Keller and Lazareva (2013), about 10–30%, 3–17%, and 4–19% of ENPs produced will be released into water bodies in Asia, Europe, and North America, respectively. One previous study (Keller et al. 2013) has estimated that 63–91% of over 260–309 thousand metric tons of global engineered nano-material production in 2010 ended up in landfills, with the balance released into soils (8–28%), water bodies (0.4–7%), and the atmosphere (0.1–1.5%). A more recent study has shown that for TiO_2-ENPs (39,000 tons/year) and Ag-ENPs (50 tons/year), about half of the year's total input into the system entered the in-use stock and the rest was directly released into environmental compartments within the same year (Sun et al. 2016). A recent review (Troester et al. 2016) has reported that the wide range of ENPs is clearly produced in the tons-per-year range and is therefore the potential to be released in significant amounts into the environment. Choi et al. indicated that the ENPs that were discharged to wastewater treatment plants, which served as redistribution points, and ultimately transferred to the aquifer were estimated at 26–39% of the total ENPs used (Choi et al. 2017). In order to assess the behavior of the released ENPs in the environment and the potential effects on organisms, it is important to know the actual form of the materials that are released (Nowack et al. 2011). The ENPs added into products or used in an application may undergo transformation and aging processes, and the released particles may be completely different from the original particles. Therefore, investigation of the amount of ENPs released and their characteristics under real-world conditions is of great importance.

Though ENPs are widely used in paints, the available studies on release in recent years mainly targeted textiles and other related consumer products (Hagendorfer et al. 2009; Kulthong et al. 2010; Lorenz et al. 2012; Windler et al. 2012; Gondikas et al. 2014). Early studies monitored the ENPs from paints released into natural waters (Kaegi et al. 2008) and investigated the leaching pattern of a certain ENP from paints under ambient conditions in a model house (Kaegi et al. 2010). Zuin et al. (2014) studied the release behavior of ENPs from paints in an immersion test. On the aspect of abrasion, there were studies on the changes of ENPs during abrasion of paint (Koponen et al. 2009; Saber et al. 2012) or the durability of ENP-containing paints (Scrinzi et al. 2011).

Previous studies on ENP-paints usually investigated the release of one type of ENP under one or two conditions in depth or aimed to estimate the amount of release (Olabarrieta et al. 2012; Al-Kattan et al. 2013, 2014a; Hincapié et al. 2015). Olabarrieta et al. (2012) analyzed the release of TiO_2-ENPs related either to the long-run performance of photocatalytic coatings or their environmental impact, and their results showed that the TiO_2 emission concentration was as high as 150.5 $\mu g\ L^{-1}$. Al-Kattan et al. in 2013 and 2014a discussed the releases of TiO_2-ENPs and SiO_2-ENPs from paints respectively, and results suggested that a low amount of Ti (0.007% of the total Ti) was released over 113 weathering cycles, while the released SiO_2-ENPs constituted 2.3% of the total SiO_2 in the paint. Hincapié et al. (2015) investigated the flows of ENPs from paints in construction and demolition waste, and they found that the majority of ENPs entered recycling systems (23 times per year), while a smaller amount was disposed directly into landfills (7 times per year) and only a tiny fraction of ENP waste was incinerated (0.01 times per year). Adeleye et al. (2016) studied the release of Cu-ENPs from a commercial antifouling paint, and they discovered that both the length of drying time and type of surface painted strongly influenced the amount of Cu released into natural waters. Information on to what extent specific factors act together and affect the concentrations of different types of ENPs released from paints applied on building panels, or how much each factor contributes in comparison with the others, was insufficient. Therefore, this study aimed to investigate factors that may influence the ENPs' release, including weathering duration, water pH, rainfall intensity, and duration, using the most frequently used ENPs in the paint industry, TiO_2-ENPs, SiO_2-ENPs, and Ag-ENPs.

Materials and methods

Paints used and applications

Pristine ENPs used in our experiments were supplied by the industry (Dekedaojin (Beijing) Co., Ltd.). The declared average size of SiO_2-ENPs (modified with coupling agent KH-550, NH_2 $(CH_2)_3Si(OC_2H_5)_3$) was 10 nm, TiO_2-ENPs (anatase, modified with coupling agent KH-550, NH_2 $(CH_2)_3Si(OC_2H_5)_3$) 30 nm, and Ag-ENPs 50 nm (Table 1). Figure 1 shows the transmission electron microscopy (TEM) images of the three pristine ENPs and their forms after being mixed in paints. Figure 2 shows the

Table 1 Properties of pristine SiO_2-, TiO_2-, and Ag-ENPs used

	Average size (nm)	Zeta potential (mV)	Dispersing agent	Hydrophobicity
SiO_2-ENPs	10	− 28 ± 1	Silane coupling agents	Hydrophilic
TiO_2-ENPs	30	− 35 ± 1	Silane coupling agent	Hydrophilic
Ag-ENPs	50	− 30 ± 1	–	Hydrophilic

scanning electron microscope (SEM) images of these three ENPs in paints. As shown in Fig. 2, SiO_2-ENPs, Ag-ENPs, and TiO_2-ENPs were all distributed evenly within the matrix and some of them within the top surface.

The paints containing ENPs were fabricated by adding a known amount of TiO_2-ENPs, SiO_2-ENPs, or Ag-ENPs directly to paints with no ENPs as described by Zuin et al. (2014), with manual stirring followed by ultrasonic treatment for 30 min. The composition of the paints used in this study is given in Table 2 (as per the manufacturer's manual), one of each containing SiO_2-ENPs (5 wt%), Ag-ENPs (1 wt%), and TiO_2-ENPs (3 wt%), respectively, plus control paints without ENPs. The TiO_2 pigment is composed of elongated particles in the range from 100 to 300 nm (provided by the paint's manufacturer).

Fiber cement panels were cut into sections with the dimensions of 50 × 70 mm^2 and 300 × 75 mm^2, which were suitable sizes for the equipment (Accelerated Weathering Tester, ZH/ZW-P, Zhichou (Shanghai) Co., Ltd.). The amount of paints used and methods of conditioning, coating, and drying of panels were adopted from a study by Zuin et al. (2014). In detail, all panels were conditioned according to the European Standard (EN, 1062-11:2002). Conditioned panels were then coated with 0.4 kg m^{-2} of wet paints in two layers. Panels including both sides and all edges were totally coated by using a brush. Painted panels were then dried for 7 days in a climatic chamber at 23 ± 2 °C with humidity of 50 ± 5%. The determination of the amount of paint applied to each panel and methods of drying were based on the paint manufacturer's recommendations.

Artificial weathering and rainfall simulation

Artificial weathering tests were performed in a weathering chamber (Accelerated Weathering Tester, ZH/ZW-P, Zhichou (Shanghai) Co., Ltd.) using a UV-A lamp (315–400 nm; 50 W m^{-2}). Up to 63 cycles of 8 h each (4 h with lamps on at $T = 60 \pm 2$ °C and 4 h off, and water condensation at $T = 50 \pm 2$ °C) was applied during the weathering process, based on ISO 11507:2007a. The weathering process was interrupted at selected times (100, 150, 200, 250, 300, 350, 400, and 500 h) for leaching analysis.

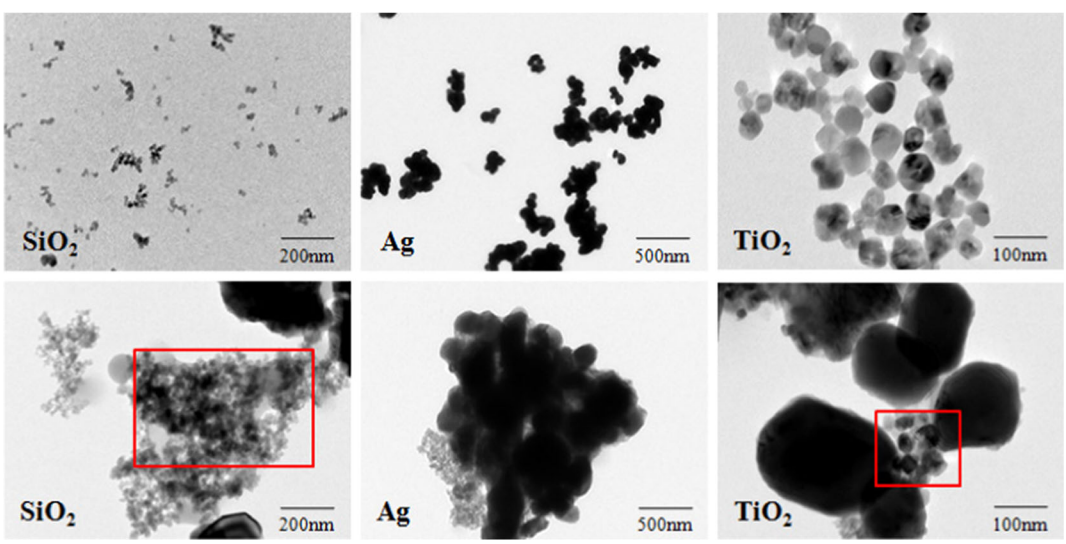

Fig. 1 The TEM images of the three types of pristine ENPs (i.e., SiO_2, Ag, and TiO_2) alone (top) and in diluted paints (bottom). Note: the red squares in two of the micrographs are used to mark SiO_2-ENPs and TiO_2-ENPs in the paints

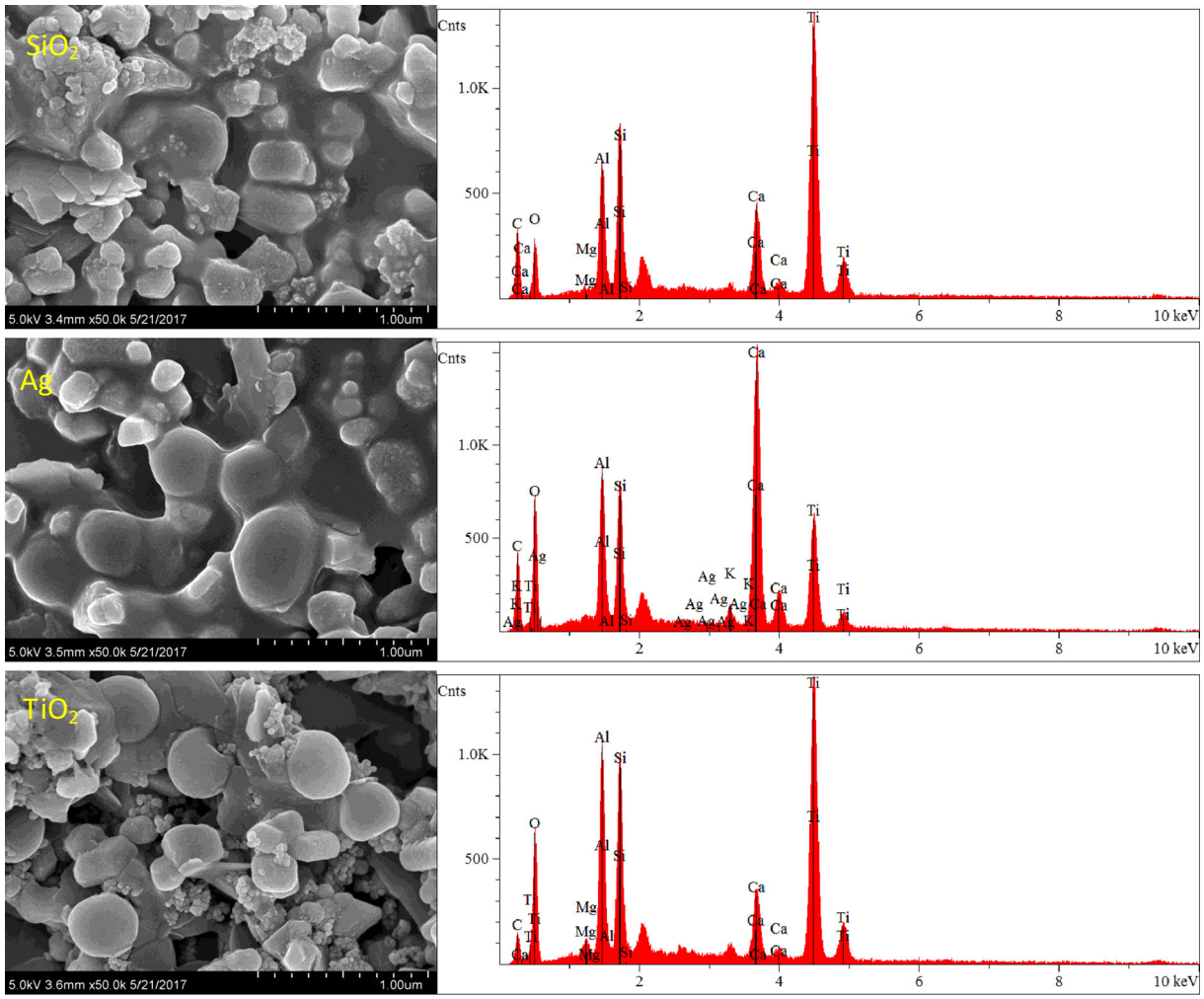

Fig. 2 The SEM images of the three types of ENPs (i.e., SiO_2, Ag, and TiO_2) distributed in paints

Table 2 Composition of the paints (wt%)

	Blank sample	Paint with SiO_2-ENPs	Paint with Ag-ENPs	Paint with TiO_2-ENPs
Water	29.80	13.13	29.80	19.80
Calcium carbonate	13	13	12	13
Wollastonite	2.1	2.1	2.1	2.1
TiO_2 pigment	16.59	16.59	16.59	16.59
Talcum	6.63	6.63	6.63	6.63
Styrene-acrylic copolymer dispersion	20	20	20	20
SiO_2-ENPs slurry (30%)	–	16.67	–	–
Ag-ENPs	–	–	1	–
TiO_2-ENPs slurry (30%)	–	–	–	10
Others (e.g., thickener, dispersant, defoamer, and preservatives)	11.88	11.88	11.88	11.88

Although natural rainwater may contain components other than water such as sulfur, nitrogen oxides, chlorine, and sodium ions, as the composition of rainwater varies by region and climate conditions, and no single composition is broadly representative, deionized water (18 MΩ cm^{-1}) was chosen in this study (pH = 7). A device was constructed to spray deionized water onto the panels. The rate of rainfall was controlled by adjusting the water pressure supplied to the nozzles. All rainfall simulations took place indoors to avoid the effects of wind or sunlight.

Leaching test and analysis

For analyzing the effect of pH and rainfall on the leaching of samples, 500 h of weathering time was chosen. UV ray exposed panels and unweathered panels were immersed in 94 mL of water, resulting in 188 cm^2 (two of the 50 × 70 × 10 mm^3 panels) of panel surface in contact with deionized water. All panels were immersed for 3/4 of their length according to the ISO 2812-2:2007b procedure, with a surface to volume ratio (S/V) = 2 (i.e., 188 cm^2 of painted panel is leached in 94 mL) in order to submerge the maximum panel surface, taking into account the different dimensions of tested panels (Zuin et al. 2014). The effect of pH was studied by varying the pH from 3 to 10. While immersing the panels in water at a particular pH, the pH was maintained with 0.5 mol L^{-1} HCl and 0.5 mol L^{-1} NaOH at 2 h intervals (not adjusted over time). To quantify the content of ENPs in the leachate, 10 mL of samples were collected after 24 h of immersion. Concentrations (μg L^{-1} or mg L^{-1}) of Si, Ag, and Ti in the static water immersion test were converted into losses per area or per mass (μg m^{-2}, mg m^{-2}, mg g^{-1}, and μg g^{-1}).

In rainfall simulation tests, treatments followed 12 + 6 factor design with 12 rainfall durations (10 to 120 min at 10 min intervals; 90 mm h^{-1}) and 6 rainfall intensities (30, 42, 60, 72, 90, and 102 mm h^{-1}) (Blaustein et al. 2015). During rainfall, 10 mL of each runoff was collected from the respective troughs at the 12 time points to analyze the effect of rainfall duration on ENP release. When studying the effect of rainfall intensities, all runoffs were collected at 60 min. All samples collected were digested with 2% HNO_3 and then analyzed by using inductively coupled plasma mass spectrometry (ICP-MS; NexION 300X, PerkinElmer).

For analyzing the size distribution of released particles, 500 h of weathering time was chosen. The ENPs in the leachates were measured with a dynamic light scattering device (Zetasizer 90, Malvern). The device was equipped with a 35 mW He-Ne laser, 633 nm laser diode and photodiode detector set at 90°. Each auto-correlation function was accumulated for 10 s, and more than 10 auto-correlations were conducted for each measurement. One milliliter of the leachate was introduced into a cuvette to determine particle size. The hydrodynamic diameter (intensity based) was calculated using the Stokes-Einstein equation. Volume distributions were obtained from the fundamental intensity distribution using Mie theory. All measurements were conducted at 25 °C, at a minimum, in duplicate.

Statistical analysis

SPSS 16.0 software was used for the statistical analysis in this study. The statistical differences among the data were analyzed by one-way analysis of variance, followed by Tukey's post hoc test at 5% level.

Results and discussion

Size distribution of released particles

The ENPs released from aged paints were characterized by a dynamic light scattering device (Zetasizer 90, Malvern) in the range between 0.01 and 10 μm. The size distribution of Si released from paint aged for 500 h is shown in Fig. 3. The SiO_2 concentration in this leachate (aged 500 h in the static water immersion test on the effect of weathering duration) was 12 mg L^{-1}, which corresponded to 0.62% of the total SiO_2 added to the paint. The Zeta potential of the SiO_2-ENPs after incorporating them into the paint formulation was − 3.83 ± 1 mV.

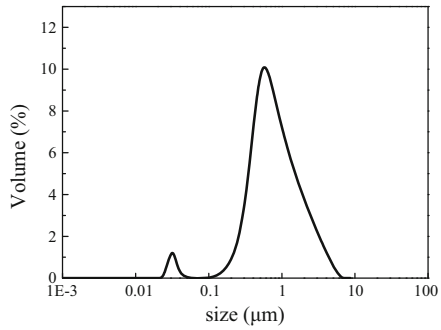

Fig. 3 Size distribution of Si released from paint after 500 h weathering

Figure 3 shows that the particle size of the released ENPs was in the range 0.03–9 μm, and the peak of the size distribution was 0.8 μm. The small peak in Fig. 3 indicates that only a small fraction of released ENPs was below 0.1 μm. Therefore, most of the Si was present in large particles rather than single SiO_2-ENPs. Ag and Ti were not detected by dynamic light scattering, which may be because the concentrations of these two particles were under the detection limit for the leachate collected.

Release of ENPs with weathering duration

As shown in Fig. 4 (a1), the concentration of Si increased from 7.5 to 12 mg L^{-1} during 500 h of weathering. As there were no added SiO_2-ENPs in the blank sample, the difference in concentration of Si between nano samples and blank samples should be associated with the added SiO_2-ENPs. The cumulative loss and fraction of Si from SiO_2-ENPs over the weathering time is displayed in Fig. 4 (a2). After 24 h in contact with water, the total loss of Si from panels with various weathering durations was 35–58 mg m^{-2}. The initial concentration of SiO_2-ENPs paint was approximately 5%, equivalent to 20 g m^{-2} of SiO_2 or 9.33 g m^{-2} of Si applied onto the panels. Therefore, the loss of Si from test panels corresponded to a loss of 0.38–0.62%.

Figure 4 (b1) shows the concentration of Ag in leachate. The Ag released from paints was very low, ranging between 21.32 and 42.16 μg L^{-1}. This phenomenon was different from the result of Kaegi et al. (2010), in which strong leaching of the Ag-ENPs was observed (with a maximum concentration of 145 μg L^{-1}). After 24 h of immersion, the per area loss of Ag from experiment panels ranged from 107 to 213 μg m^{-2}, equivalent to a mass release per mass of paint applied from 0.09 to 0.15 mg g^{-1} (corresponding to a loss of 0.025‰ to 0.055‰) (Fig. 4 (b2)).

As seen in Fig. 4 (c1), Ti released from paints was always below 2.4 μg L^{-1} in the leachate. ICP-MS measurements of this particle also showed an overall increase of Ti content. With 12 g m^{-2} of TiO_2-ENPs applied onto the panels, the loss of Ti from panels reached 5.76 μg m^{-2}, equivalent to 0.014 μg g^{-1} (corresponding to a loss of 0.00048‰) after 500 h of weathering (Fig. 4 (c2)). Despite the deterioration by weathering, the TiO_2-ENP coated sample surfaces were still strong enough to resist leaching of the constituent ENPs into the water. A study conducted by Al-Kattan et al. (2013) showed that the amount of bulk particles released from paints was below 2 μg L^{-1}, which is similar to the nanoparticle release in the present study (< 2.4 μg L^{-1}).

The released amounts of the three types ENPs all increased with weathering duration (Fig. 4). In terms of mass leached per area, the release was generally linear with weathering, which may be due to the presence of cracks on the surface of panels. The significant release without weathering is perhaps due to the direct release of ENPs from the surface of the paint. Lebow et al. (2003) showed that initial leaching reflected the loss of poorly fixed or readily available components. A higher concentration of Si released from the panels was observed, accompanied by a higher density of cracks in the panel surface containing SiO_2-ENPs than for Ag- and TiO_2-ENPs (Fig. 5). Surface cracks from the combined effect of UV degradation and wetting and drying cycles may have increased the paint surface area and provided the mechanism for the increased leaching of ENPs (Lebow et al. 2003). The density of cracks may be attributed to cross-linking reactions as well as the effect of SiO_2-ENPs on these reactions (Ranjbar and Rastegar 2009). As Ranjbar and Rastegar (2009) reported, the incorporation of SiO_2-ENPs may result in side reactions, which could change the distribution of the cross-links throughout the polymeric matrix. The cross-linking reactions by poly-condensation could result in volume reduction, with the shrinkage being more intensive in the neighborhood of SiO_2-ENPs.

Release of ENPs under different pH

The effects of pH on the release of ENPs from panels after 24 h of immersion (note: the panels were aged for 500 h before immersion) are shown in Fig. 6. SiO_2-ENPs bound to the panels were relatively stable at pH 4 to 8, and their release was on average 13.19 mg L^{-1} (Fig. 6 (a1)). Outside this pH range, the release of Si increased to above 15 mg L^{-1} as pH went lower or higher. When converted into cumulative and percentage losses, the release pattern versus pH is more obvious (Fig. 6 (a2)). The pattern may be due to the stronger activity of Si at low or high pH. Although the SiO_2-ENPs used in this study were modified by silane coupling agents (KH-550, $NH_2(CH_2)_3Si(OC_2H_5)_3$), not all of the silanol groups on the surface of the SiO_2 particles reacted with them (Chen et al. 2005). At high pH, protons from the surface silanol groups from the unmodified silica sites are dissociated ($-SiOH + OH^- \rightarrow -SiO^- + H_2O$). At low pH, most of the negative

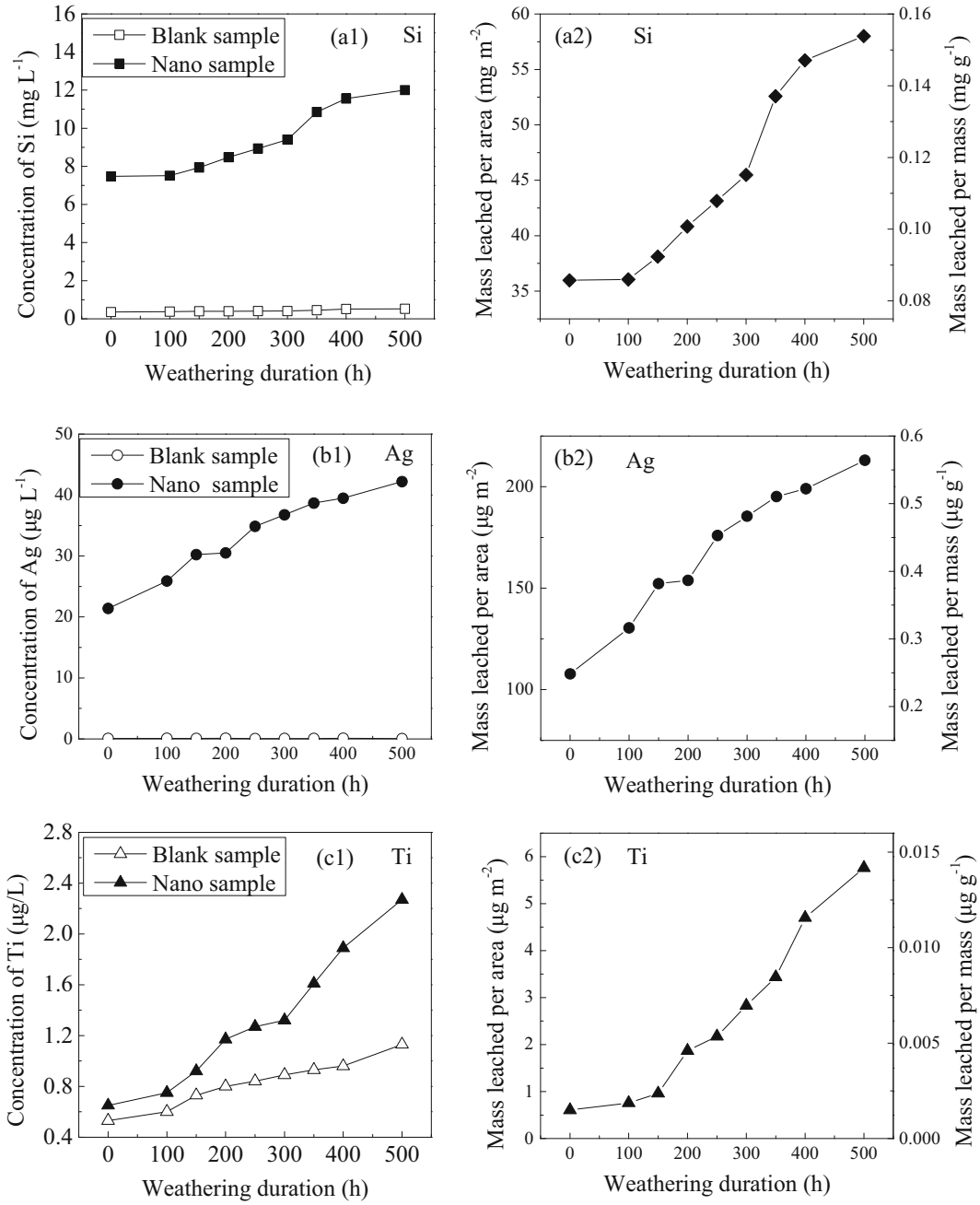

Fig. 4 The concentration of released ENPs with different weathering durations

groups are protonated by the abundant H^+ ions in solution. After modification, amines can be introduced (Chen et al. 2005). The silica particles modified with amino silane are also active at low or high pH values, as the amino groups could protonate at low pH value and deprotonate at high pH value ($-NH_2 + H^+ \rightarrow -NH^+$; $-NH_2 + OH^- \rightarrow -NH^- + H_2O$) (Pham et al. 2007).

As seen in Fig. 6 (b1), the release of Ag displays a similar pattern to that of Si, with the average release at 41.75 μg L^{-1} between pH 4 to 8. Below pH 4, the release of Ag increased as pH decreased, which may be due to the faster dissolution of Ag at low pH (Peretyazhko et al. 2014). Peretyazhko et al. (2014) have shown that the extent of Ag-ENP dissolution in acid was larger than in

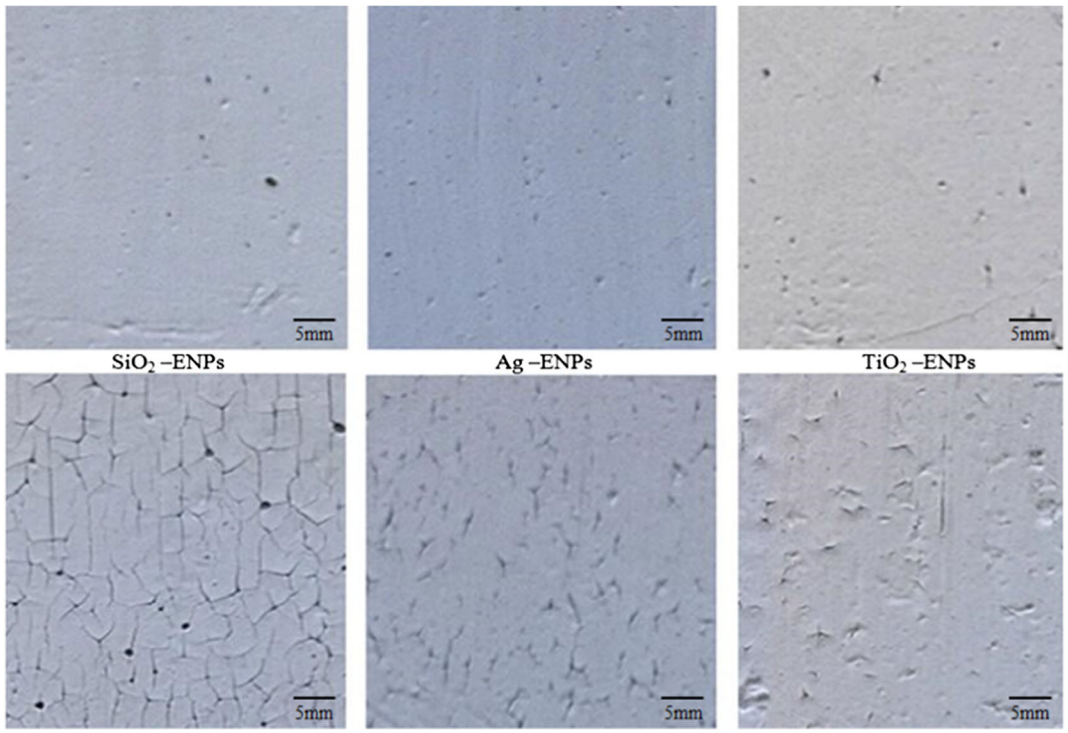

Fig. 5 Contrasting pictures of panels before (top) and after 500 h of weathering (bottom)

water. On the other hand, it may also be attributed to the interaction between water and the Ag surface at low pH. According to Li et al. (2010), interaction between water and the metal surface could cause the redshifting of O–H stretching frequencies. The negative surface charge favors the binding of the H-end of water to the nanoparticle electrode surface, forming the HO–H…Ag hydrogen bond. In acidic solutions, the surface species exist in the form of hydrated proton clusters, such as H_3O^+, $H_5O_2^+$, $H_7O_3^+$, or $H_9O_4^+$. When a negative potential was employed, the hydrated proton clusters strongly interacted with the nanoparticle electrode surface. Therefore, it may be concluded that at low pH, Ag tended to be hydrophilic. In addition, the lowest loss was observed at pH 8, but increased as pH was raised above this level. This may be explained by the fact that the concentration of the nanoparticle surface electrons of the metal cathode rises with increasing pH, resulting in a large effective polarizability and a reaction with water as follows: $e + H_2O \rightarrow H_{ad} + OH^-$ (Li et al. 2010). When taking into account the proportions of the panels and weight of the paint applied, 266 μg m^{-2} and 264 μg m^{-2}, corresponding to 0.67 μg g^{-1} and 0.66 μg g^{-1} of the released Ag, was observed at pH 3 and 10, respectively (Fig. 6 (b2)).

The release of Ti as a function of pH exhibits a different pattern from those of Si and Ag (Fig. 6 (c)). The concentration of Ti release is at similar low levels at pH 3 and 10, while at high level at pH 6 (i.e., 3 μg L^{-1}), followed by a sharp decline to the lowest level of 1 μg L^{-1} at pH 7. This special phenomenon may be associated with the photocatalytic activity of TiO_2-ENPs. As Amy et al. (1995) reported, TiO_2-ENPs are semiconductors, the valence electrons of which can be injected into the conduction band and form holes under irradiation by 400 nm UV light. When the holes are in contact with water, H^+ can be reduced to H_2. After ultraviolet aging, TiO_2-ENPs may become more active at low pH values and tend to be in contact with water. In addition, the sharp decline at pH 7 may be attributed to the electrostatically unfavorable conditions of TiO_2-ENPs at neutral pH (Chowdhury et al. 2011).

As seen in Figs. 4 and 6, except for Ti, in the studied conditions, the effect of pH on the release of Si (p = 2.73e−06 < 0.05) and Ag (p = 1.70e−03 < 0.05) is larger than that of weathering. However, in natural conditions, the exposure time of the paints to air would be far longer than the study time, and the aging conditions may also be greater than the experimental

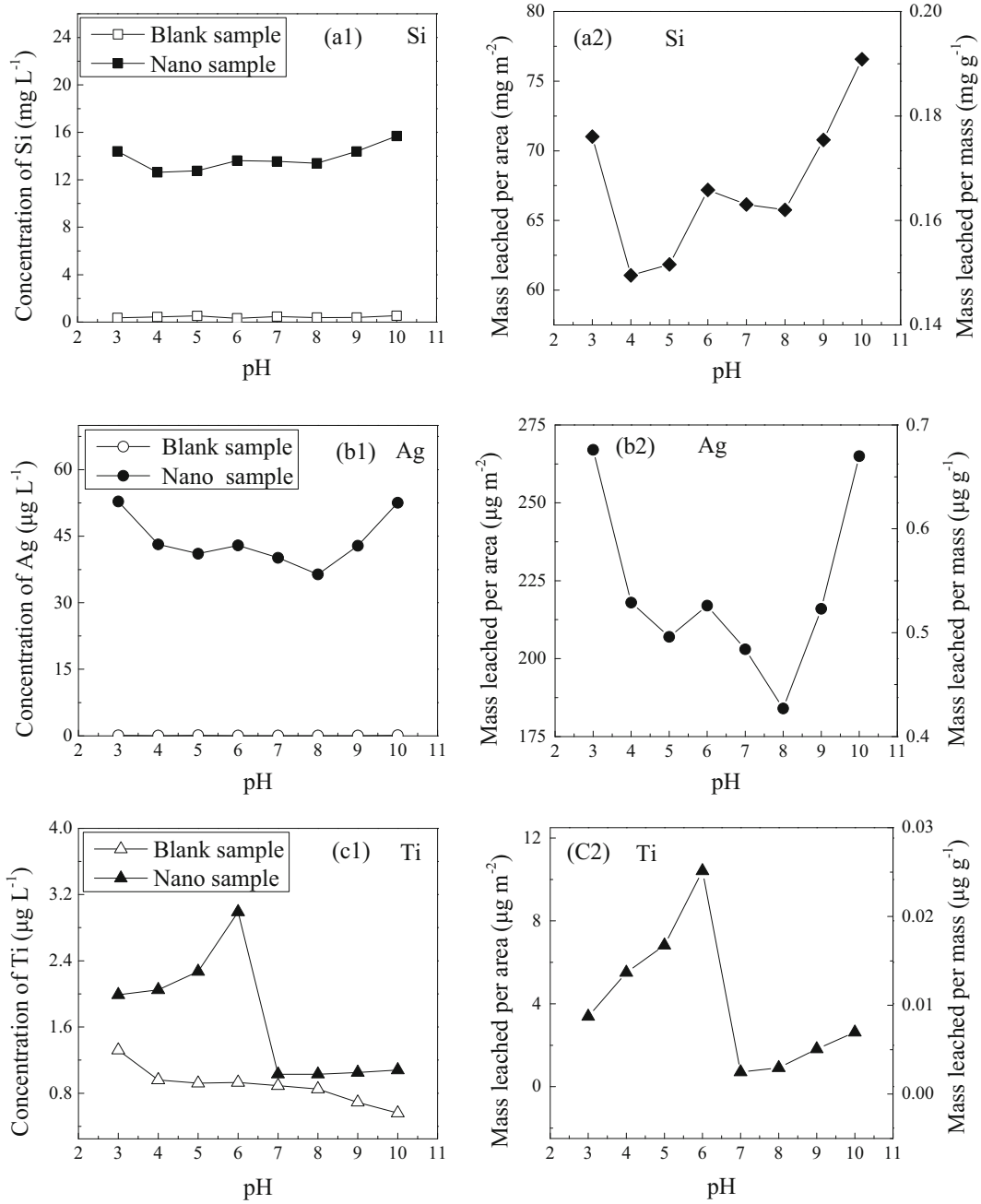

Fig. 6 The concentration of released ENPs with different water pH

conditions. However, the pH of rain water is rarely lower than 3 or higher than 10 (Tang et al. 2005; Zhang et al. 2007), and thus, the effect of rainfall pH on particle release from paints may not be greater than found in this study. Considering all these factors, the effect of weathering time may be greater than that of pH on particle release in the long run.

Release of ENPs with different rainfall conditions

Release of ENPs with different rainfall durations

In this study, the leaching tests for the three ENPs with different rainfall durations show distinct concentration profiles (Fig. 7). The concentration of Si in the leachates

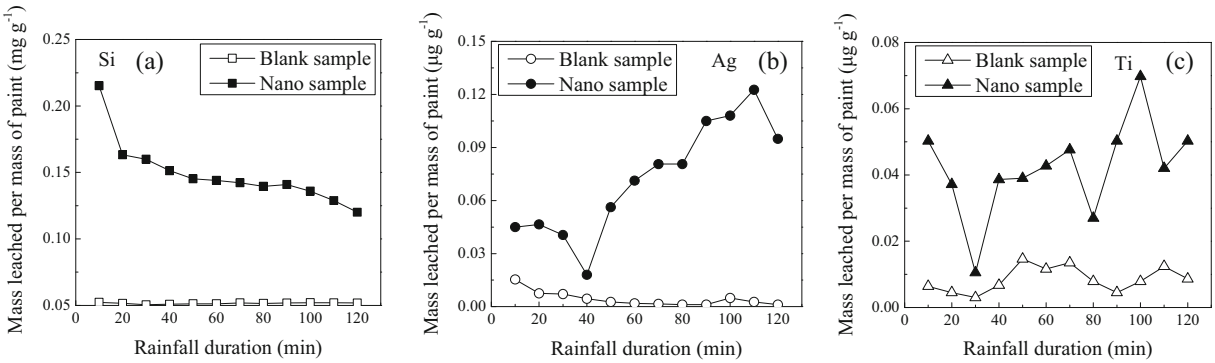

Fig. 7 The concentration of released ENPs with different rainfall duration

is initially high (0.22 mg g^{-1}) and then decreases only slightly from 0.16 to 0.13 mg g^{-1} between 20 and 120 min (Fig. 7 (a)). This observation may be accounted for by the higher volume of water that resulted from a longer rainfall duration. With longer duration, the released particles would be diluted more than with a shorter duration. A concern with SiO_2-ENPs in paint is that the binder will gradually lose its ability, and over time, the concentration in the leachates might increase to levels similar to that of initial release (Lebow et al. 2003).

The release of Ag generally shows an increase between 40 and 110 min from 0.02 to 0.12 μg g^{-1} (Fig. 7 (b)), except for the rainfall before 40 and after 110 min. Possible explanations may be due to rainfall erosion leading to the organic binder being less sticky. As a result, with longer duration, more and more Ag-ENPs were transformed into other forms with decreased binding ability to the organic binder. In addition, Schnippering et al. (2007) reported that Ag could rapidly oxidize when exposed to air, suggesting that the pattern of Ag-ENPs may reflect the properties of the oxidized form.

The concentration of Ti also decreased initially (in the initial 10–30 min), and mostly fluctuated between 0.03 and 0.05 μg g^{-1} afterwards. The exceptions of the trend are at 30, 80, and 100 min. Overall, no correlation between Ti concentration and rainfall duration was observed (Fig. 7 (c)). Except for the poorly fixed particles, this phenomenon may be explained by the varying status of TiO_2-ENPs in the paints. As described in a previous study, TiO_2-ENPs may be immobilized on the surface of paints in two ways: one involves the formation of a relatively stable chemical structure resulting from the reaction between TiO_2-ENP particles and functional groups in the polymer, such as C=O in styrene-acrylic copolymer; the other involves embedding of TiO_2-ENP particles in the paints as a result of their intertwining with polymer chains during the paint preparation process (Bian et al. 2011). These various states may lead to different adhesive abilities of TiO_2-ENPs to paints, and thus, the concentration of Ti released with rainfall duration is hard to predict.

Release of ENPs with different rainfall intensity

As shown in Fig. 8a, the release of Si shows an increasing tendency. The increased runoff contribution in the Si release as the rainfall intensity increased may be related to positive effects of rainfall intensity on the sloughing of relatively large SiO_2-ENPs particles. In addition, the release of Si from paints is significantly higher than the release of Ag and Ti, which may be explained by the high density of cracks present on the surface of panels. SiO_2-ENPs located beside these cracks may be poorly fixed and could easily be washed away under rainfall events.

The release of Ag with rainfall intensity is similar to that of Si (Fig. 8b). At 102 mm h^{-1}, the release of Ag is the highest, at 0.2 μg g^{-1}, followed by the value at 90 mm h^{-1}. Although an increasing tendency is shown in total, the release content of Ag in medium rainfall intensity (42, 60, 72, and 90 mm h^{-1}) is similar (0.07–0.09 μg g^{-1}). Initial leaching reflects the loss of poorly fixed or readily available components.

For Ti, the release content with rainfall intensity also shows an increase trend and is almost linear. In addition, similar to Si and Ag, the highest rainfall intensity (102 mm h^{-1}) generated the highest release concentration at 28 ng g^{-1}, followed by 90 mm h^{-1} at 25 ng g^{-1}, while the low rainfall intensities (30 mm h^{-1} and 42 mm h^{-1}) developed the lowest concentrations, at around 4 ng g^{-1} (Fig. 8c).

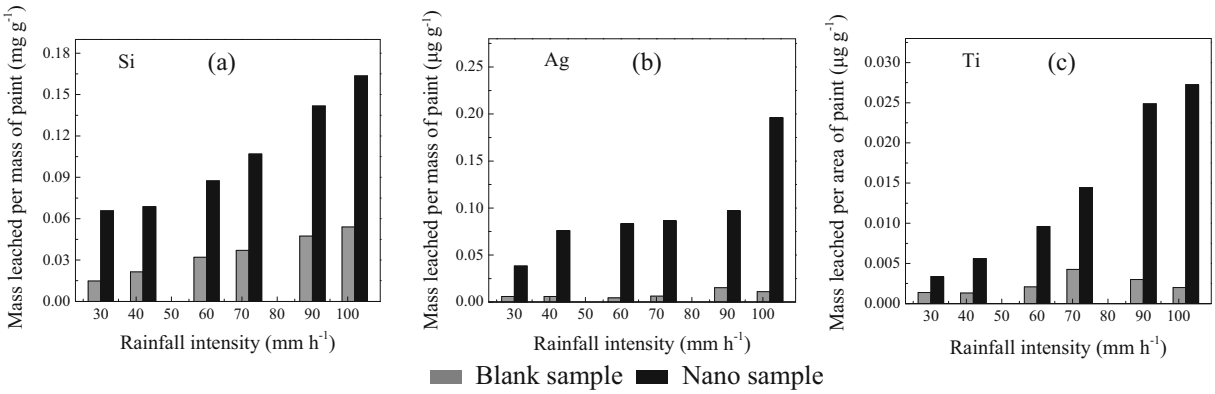

Fig. 8 The concentration of released ENPs with different rainfall intensities

The differences among the releases of these three particles from panels under simulated rainfall intensities on the one hand may be due to the differing densities of cracks present on the surfaces (Fig. 5); on the other hand, they may be attributed to the different adhesion abilities of ENPs applied to the paints. As Yang et al. (2015) discussed, the ENPs in the bilayer membrane were probably in contact with a patch of the membrane or only a few polymer chains, which was mainly determined by the sizes and shapes of the ENPs. This contact situation influences the ENP-membrane binding and the configuration change of the polymer chains, and the competition between these factors determines the final adhesion state of the ENPs on the membrane. In this study, some SiO_2-ENPs appeared as rod-like particles, and some as ellipses (Fig. 9), while most of Ag-ENPs and TiO_2-ENPs were ellipses (Fig. 1). A previous study mentioned that ellipsoid-like ENPs facilitated particle-polymer binding and the consequent adhesion between them (Yang et al. 2015), whereas rod-like ENPs with squarish cross-section indenters have much larger detachment loads than circular ones (Sundaram and Chandrasekar 2011).

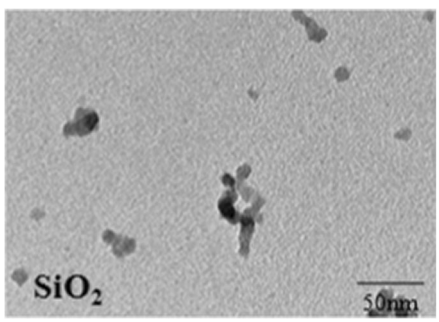

Fig. 9 The TEM images of SiO_2-ENPs

In the rainfall erosion test, except for Ag, the effect of rainfall duration on the release of Si (p = 2.11e−02 < 0.05) and Ti (p = 2.40e−02 < 0.05) was larger than that of rainfall intensity. Similar to the effect of weathering time, the rainfall durations under real conditions display a large range of variation and are often longer than 2 h, and thus, more particles may be released than in this study. On the contrary, the variation of rainfall intensity is limited. According to DB11/T 685-2009, the rainfall intensity most of the time is less than 100 mm h^{-1}, and several levels were tested up to 102 mm h^{-1} in this study, so the effect of rainfall duration on particle release from paints in this study may be greater than the effect of rainfall intensity under real conditions.

Overall, the release of Ag and Ti in our study was low, especially for Ti. Besides the reasons discussed above, the weathering time studied may still not be long enough. Our work has only targeted the short-term behavior of release and stability. The long-term fate of the particles may be governed by the fate of the matrix, which in our case is the styrene-acrylic copolymer binder. If this material is chemically or photochemically degraded, then free ENPs could be released. The added TiO_2-ENPs are photochemically active, and further degradation of the paint matrix is possible under light exposure, resulting in the release of particles (Al-Kattan et al. 2014b).

Conclusion

The release of SiO_2-ENPs, Ag-ENPs, and TiO_2-ENPs from experimental paints as affected by various factors (i.e., weathering duration, pH, rain duration, and

intensity) was investigated by laboratory testing of facade coatings. With weathering durations up to 500 h, the concentration of Si release (i.e., 7.5–12 mg L^{-1}) was much higher than Ag and Ti (i.e., 21.32–42.16 μg L^{-1} and 0.6–2.3 μg L^{-1}, respectively). However, only a small fraction of Si was released in ENP form, and the particle size distribution for Ag and TiO_2 was under the detection limit. Regarding the effect of pH, SiO_2-ENPs and Ag-ENPs showed higher release at low and high pH values, while the release of TiO_2-ENPs was relatively higher at low pH, and these phenomena may be attributed to the activity of ENPs at different pH values. In the rainfall simulation tests, with rainfall duration, the concentrations released into water increased for SiO_2-ENPs, decreased for Ag-ENPs, and displayed no regular patterns for TiO_2-ENPs. As for the rainfall intensity, Si, Ag, and Ti all exhibited an increasing tendency with rainfall intensity. When considering these influence factors together, conclusions may be reached that weathering time and rainfall durations tended to have greater effects on release than water pH and rainfall intensity.

Acknowledgments This research was supported by the Scientific Research Project of Beijing Educational Committee (SQKM201710016016), Beijing Outstanding Talent Project for Excellent Youth Team (2015000026833T0000), Pyramid Talent Cultivation Project of Beijing University of Civil Engineering and Architecture, Beijing Advanced Innovation Center for Future Urban Design: Sponge City Development and Water Quantity & Quality Risk Control (UDC2016040100), The Importation and Development of High-Caliber Talents Project of Beijing Municipal Institutions.

Compliance with ethical standards

Conflict of interest The authors declare that they have no conflict of interest.

References

Adeleye AS, Oranu EA, Tao M, Keller AA (2016) Release and detection of nanosized copper from a commercial antifouling paint. Water Res 102:374–382

Al-Kattan A, Wichser A, Vonbank R, Brunner S, Ulrich A, Zuin S, Nowack B (2013) Release of TiO_2 from paints containing pigment-TiO_2 or nano-TiO_2 by weathering. Environ Sci Process Impacts 15(12):2186–2193

Al-Kattan A, Wichser A, Vonbank R, Brunner S, Ulrich A, Zuin S, Arroyo Y, Golanski L, Nowack B (2014a) Characterization of materials released into water from paint containing nano-SiO_2. Chemosphere 119:1314–1321

Al-Kattan A, Wichser A, Zuin S, Arroyo Y, Golanski L, Ulrich A, Nowack B (2014b) Behavior of TiO_2 released from nano-TiO_2-containing paint and comparison to pristine nano-TiO_2. Environ Sci Technol 48(12):6710–6718

Alvarez PJ, Colvin V, Lead J, Stone V (2009) Research priorities to advance eco-responsible nanotechnology. ACS Nano 3(7): 1616–1619

Amy L, Linsebigler GL, John T, Yates J (1995) Photocatalysis on TiO_2 surfaces: principles, mechanisms, and selected results. Chem Rev 95:735–758

Beijing Municipal Bureau of Quality and Technical Supervision. (2009) DB11/T 685-2009 technical code on rainwater harvesting engineering in urban area

Bian X, Shi L, Yang X, Lu X (2011) Effect of nano-TiO_2 particles on the performance of PVDF, PVDF-g-(maleic anhydride), and PVDF-g-poly(acryl amide) membranes. Ind Eng Chem Res 50(21):12113–12123

Blaustein RA, Pachepsky YA, Hill RL, Shelton DR (2015) Solid manure as a source of fecal indicator microorganisms: release under simulated rainfall. Environ Sci Technol 49(13):7860–7869

Chen G, Zhou S, Gu G, Yang H, Wu L (2005) Effects of surface properties of colloidal silica particles on redispersibility and properties of acrylic-based polyurethane/silica composites. J Colloid Interface Sci 281(2):339–350

Choi S, Johnston MV, Wang GS et al (2017) Looking for engineered nanoparticles (ENPs) in wastewater treatment systems: qualification and quantification aspects [J]. Sci Total Environ 590-591:809–817

Chowdhury I, Hong Y, Honda RJ, Walker SL (2011) Mechanisms of TiO_2 nanoparticle transport in porous media: role of solution chemistry, nanoparticle concentration, and flowrate. J Colloid Interface Sci 360(2):548–555

European Committee for Standardization (CEN) (2002) EN 1062-11:2002 paint and varnish: coating materials and coating systems for exterior masonry and concrete. Part 11: methods of conditioning before testing. CEN, San Diego

Gondikas AP, von der Kammer F, Reed RB, Wagner S, Ranville JF, Hofmann T (2014) Release of TiO_2 nanoparticles from sunscreens into surface waters: a one-year survey at the old Danube recreational Lake. Environ Sci Technol 48(10):5415–5422

Hagendorfer H, Lorenz C, Kaegi R, Sinnet B, Gehrig R, Goetz NV, Scheringer M, Ludwig C, Ulrich A (2009) Size-fractionated characterization and quantification of nanoparticle release rates from a consumer spray product containing engineered nanoparticles. J Nanopart Res 12(7):2481–2494

Hincapié I, Caballero-Guzman A, Hiltbrunner D, Nowack B (2015) Use of engineered nanomaterials in the construction industry with specific emphasis on paints and their flows in construction and demolition waste in Switzerland. Waste Manag 43(3):451–455

International Organization for Standardization (ISO). (2007a) ISO 11507:2007 paints and varnishes: exposure of coatings to artificial weathering: exposure to fluorescent UV lamps and water. ISO, Geneva

International Organization for Standardization (ISO). (2007b) ISO 2812-2:2007 Paints and varnishes: determination of resistance to liquids. Part 2: water immersion test. ISO, Geneva

Kaegi R, Ulrich A, Sinnet B, Vonbank R, Wichser A, Zuleeg S, Simmler H, Brunner S, Vonmont H, Burkhardt M,

Boller M (2008) Synthetic TiO_2 nanoparticle emission from exterior facades into the aquatic environment. Environ Pollut 156(2):233–239

Kaegi R, Sinnet B, Zuleeg S, Hagendorfer H, Mueller E, Vonbank R, Boller M, Burkhardt M (2010) Release of silver nanoparticles from outdoor facades. Environ Pollut 158(9):2900–2905

Kai S, Alenius H, Norppa H, Pylkkänen L, Tuomi T, Kasper G (2010) Risk assessment of engineered nanomaterials and nanotechnologies—a review. Toxicology 269(2–3):92–104

Keller AA, Lazareva A (2013) Predicted releases of engineered nanomaterials: from global to regional to local. Environ Sci Technol Lett 1:65–70

Keller AA, McFerran S, Lazareva A, Suh S (2013) Global life-cycle releases of engineered nanomaterials. J Nanopart Res 15:1692

Khanna AS (2008) Nanotechnology in high performance paint coatings. Asian J Exp Sci 21:25–32

Koponen IK, Jensen KA, Schneider T (2009) Sanding dust from nanoparticle-containing paints: physical characterisation. J Phys Conf Ser 151:374–380

Kulthong K, Srisung S, Boonpavanitchakul K, Kangwansupamonkon W, Maniratanachote R (2010) Determination of silver nanoparticle release from antibacterial fabrics into artificial sweat. Part Fibre Toxicol 7(7):206–212

Lebow S, Williams RS, Lebow P (2003) Effect of simulated rainfall and weathering on release of preservative elements from CCA treated wood. Environ Sci Technol 37(18):4077–4082

Li JF, Huang YF, Duan S, Pang R, Wu DY, Ren B, Xu X, Tian ZQ (2010) SERS and DFT study of water on metal cathodes of silver, gold and platinum nanoparticles. PCCP 12(10):2493

Lorenz C, Windler L, von Goetz N, Lehmann RP, Schuppler M, Hungerbuhler K, Heuberger M, Nowack B (2012) Characterization of silver release from commercially available functional (nano) textiles. Chemosphere 89(7):817–824

Majestic BJ, Erdakos GB, Lewandowski M, Oliver KD, Willis RD, Kleindienst TE, Bhave PV (2010) A review of selected engineered nanoparticles in the atmosphere: sources, transformations, and techniques for sampling and analysis. Int J Occup Environ Health 16(4):488–507

Mitrano DM, Motellier S, Clavaguera S, Nowack B (2015) Review of nanomaterial aging and transformations through the life cycle of nano-enhanced products. Environ Int 77:132–147

Nowack B, Ranville JF, Diamond S, Gallego-Urrea JA, Metcalfe C, Rose J, Horne N, Koelmans AA, Klaine SJ (2011) Potential scenarios for nanomaterial release and subsequent alteration in the environment. Environ Toxicol Chem 31(1):50–59

Olabarrieta J, Zorita S, Peña I, Rioja N, Monzón O, Benguria P, Scifo L (2012) Aging of photocatalytic coatings under a water flow: long run performance and TiO_2 nanoparticles release. Appl Catal B Environ 123–124(4):182–192

Peretyazhko TS, Zhang QB, Colvin VL (2014) Size-controlled dissolution of silver nanoparticles at neutral and acidic pH conditions: kinetics and size changes. Environ Sci Technol 48:11954–11961

Pham KN, Fullston D, Sagoe-Crentsil K (2007) Surface charge modification of nano-sized silica colloid. Aust J Chem 60:662–666

Piccinno F, Gottschalk F, Seeger S, Nowack B (2011) Industrial production quantities and uses of ten engineered nanomaterials in Europe and the world. J Nanopart Res 14(9):1–11

Ranjbar Z, Rastegar S (2009) The influence of surface chemistry of nano-silica on microstructure, optical and mechanical properties of the nano-silica containing clear-coats. Prog Org Coat 65(1):125–130

Saber AT, Koponen IK, Jensen KA, Jacobsen NR, Mikkelsen L, Møller P, Loft S, Vogel U, Wallin H (2012) Inflammatory and genotoxic effects of sanding dust generated from nanoparticle-containing paints and lacquers. Nanotoxicology 6(7):776–788

Schnippering M, Carrara M, Foelske A, Kötz R, Fermín DJ (2007) Electronic properties of Ag nanoparticle arrays. A Kelvin probe and high resolution XPS study. PCCP 9(6):725–730

Scrinzi E, Rossi S, Kamarchik P, Deflorian F (2011) Evaluation of durability of nano-silica containing clear coats for automotive applications. Prog Org Coat 71:384–390

Sun TY, Bornhoft NA, Hungerbuhler K, Nowack B (2016) Dynamic probabilistic modeling of environmental emissions of engineered nanomaterials. Environ Sci Technol 50(9):4701–4711

Sundaram N, Chandrasekar S (2011) Shape and eccentricity effects in adhesive contacts of rodlike particles. Langmuir 27(20):12405–12410

Tang A, Zhuang G, Wang Y, Yuan H, Sun Y (2005) The chemistry of precipitation and its relation to aerosol in Beijing. Atmos Environ 39(19):3397–3406

Troester M, Brauch HJ, Hofmann T (2016) Vulnerability of drinking water supplies to engineered nanoparticles [J]. Water Res 96:255

Wiesner MR, Lowry GV, Jones KL, Jr HM, Di GR, Casman E, Bernhardt ES (2009) Decreasing uncertainties in assessing environmental exposure, risk, and ecological implications of nanomaterials. Environ Sci Technol 43(17):6458–6462

Windler L, Lorenz C, von Goetz N, Hungerbuhler K, Amberg M, Heuberger M, Nowack B (2012) Release of titanium dioxide from textiles during washing. Environ Sci Technol 46(15):8181–8188

Yang H, Wang L, Yuan B, Yang K, Ma Y (2015) Adhesion of an ultrasmall nanoparticle on a bilayer membrane is still size and shape dependent. J Mater Sci Technol 31(6):660–663

Zhang GS, Zhang J, Liu SM (2007) Chemical composition of atmospheric wet depositions from the Yellow Sea and East China Sea. Atmos Res 85(1):84–97

Zuin S, Gaiani M, Ferrari A, Golanski L (2014) Leaching of nanoparticles from experimental water-borne paints under laboratory test conditions. J Nanopart Res 16(16):1–17